Estimation and Detection for Molecular MIMO Communications in the Internet of Bio-Nano Things

O. Tansel Baydas, *Student Member, IEEE,* Oktay Cetinkaya, *Senior Member, IEEE,* Ozgur B. Akan, *Fellow, IEEE*

***Abstract*—For the Internet of Bio-Nano Things (IoBNT) applications demanding high transmission rates, a well-modeled Molecular Communication (MC) channel is essential. The existing studies proposing multiple-input and multiple-output (MIMO) models for MC, however, often make the unrealistic assumption of using ideal receivers with perfect absorption. Hence, this paper proposes a molecular MIMO channel model with spherical transmitters and partially-absorbing ligand receptor-based receivers underpinned by four unique parameters. For the non-analytical nature of the MIMO channel, we use a supervised learning algorithm to estimate the number of molecules in the reception space. We evaluate the root mean square error (RMSE) of our solution, which returns consistent results. The estimation is used for ligand-receptor binding statistics, in which the inter-symbol inference (ISI) and molecular interference are considered. We also propose two techniques based on convolutional and recurrent neural networks (CNN & RNN) as alternatives to the generic threshold-based detection. Our detectors outperform the threshold-based technique; specifically, the CNN-based method improves the mean bit error rate (BER) performance three times.**

***Index Terms*—Molecular Communication, MIMO, Channel Model, Ligand Receptors, Machine Learning, Detection.**

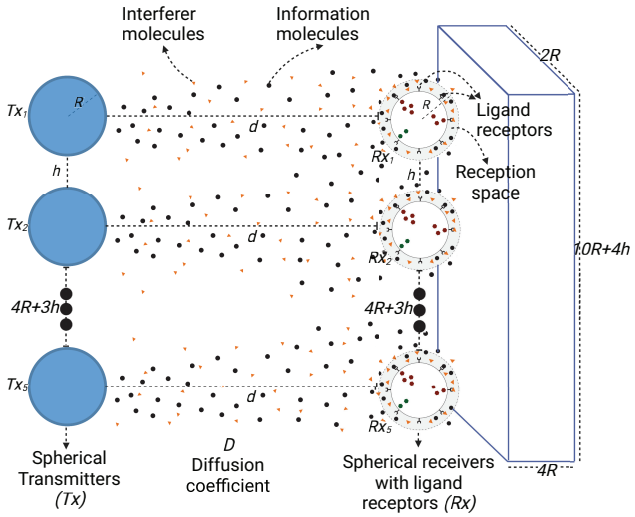

Fig. 1: Molecular MIMO channel model.

I. Introduction

Internet of Bio-Nano Things (IoBNT), built upon the communication networks of nanomachines and biological entities, is promising for novel applications, e.g., smart drug delivery and continuous health monitoring [1], for which Molecular Communication (MC) has emerged as a key enabler. MC uses molecules to transfer information, which can be encoded into the concentration or type of molecules [2]. Concentration-based MC is widely used due to its simplicity; however, the stochastic nature of Brownian motion makes it susceptible to inter-symbol interference (ISI), severely degrading the MC systems' performance. Therefore, modeling the number of received molecules is crucial for an accurate MC channel and hence for the development of the required equipment.

The research in this area first focused on estimating the single-input and single-output (SISO) MC channels. In [3], the authors proposed a spherical receiver absorbing the molecules in a cone with a fixed angle. As a data-driven approach, Machine Learning (ML) techniques were used for a similar receiver-transmitter pair with compensation parameters [4]. Furthermore, the authors in [5] designed an Artificial Neural Network (ANN)-based receiver, which achieved the same performance as a receiver with complete knowledge of the underlying channel model. Then, the multiple-input and multiple-output (MIMO) channels received attention. In [6], a 2×2 MIMO channel was analyzed, where the authors used an ANN to estimate the response of a channel with perfectly absorbing receivers. Since accurate detection of the transmitted message is unfeasible at low transmission intervals, [7] proposed Sliding Bidirectional Recurrent Neural Networks (SBRNN), to detect data sequences in consideration of the ISI.

Although most studies focus on MC detection, they consider a particular receiver that can count every molecule inside its reception space [8]. Contrarily, recent efforts propose MC receivers with ligand receptors that chemically interact with information molecules through ligand-receptor binding reactions [9]. In one of our previous works, for example, we investigated four detection methods for ligand receptors, where the interferer molecules having similar receptor-binding characteristics with the information molecules were considered [10].

Regarding all, this paper proposes a molecular MIMO channel model with spherical transmitters and ligand receptor-based receivers to achieve increased data rates, improved reliability, and enhanced capacity as against SISO systems. Compared to current literature, our model is more attainable thanks to the partially absorbing reception space with biocompatible ligand receptors. Furthermore, the received signal analysis we

O. T. Baydas, O. Cetinkaya and O. B. Akan are with the Center for neXt-generation Communications (CXC), Department of Electrical and Electronics Engineering, Koç University, Istanbul 34450, Turkey (e-mail: osman.baydas@boun.edu.tr, {ocetinkaya, akan}@ku.edu.tr).

O. B. Akan is also with the Internet of Everything (IoE) Group, Electrical Engineering Division, Department of Engineering, University of Cambridge, Cambridge CB3 0FA, UK (e-mail: oba21@cam.ac.uk).

This work was supported by AXA Research Fund (AXA Chair for Internet of Everything at Koç University).

performed is based on our previous work deriving a SISO model [11], in which the receiver absorbs the molecules within a cone with a specific angle, and particle swarm optimization (PSO) finds the unique model parameters. Besides the analytical expression, here we used a supervised ML algorithm, namely a regression tree, enhancing our model for the effects of having multiple receivers (Sec. II). Considering the ISI and molecular interference due to molecules similar to information transmitters, the bound receptors' statistics were derived using the estimated number of received molecules (Sec. III). We also compared the generic threshold-based detection with the techniques we proposed, which are based on convolutional and recurrent neural networks (CNN & RNN), in terms of bit error rate (BER) performances (Sec. IV).

II. System Model

This section first describes the MIMO channel model with analytical and ML-based estimation techniques for the number of received molecules, besides the ligand-receptor binding statistics. It then provides the details of the generated dataset that is required to apply our solution and its analysis.

A. The Ligand Receptor-based Molecular MIMO Channel

As Fig. 1 shows, our model consists of N spherical receivers (Rxs) and transmitters (Txs) deployed in a medium with a diffusion coefficient of D. The Rxs are assumed to have a radius of R, a reception space of volume V around their lipid membrane, and a separation distance of h from their nearest neighbor. We also assume that Txs are perfectly aligned with Rxs at a distance of d. The reception space is modeled to be partially absorbing at an angle of reception, β.

For the ideal SISO case assuming full absorption, the fraction of molecules entering the reception space till time t is [4]:

$$F(t) = \frac{R}{d+R} \times \text{erfc}\left(\frac{d}{y}\right), \text{and } y = \sqrt{4Dt}, \tag{1}$$

where erfc$(\cdot)$ is the complementary error function. However, (1) returns inaccurate results, i.e., high RMSE, for small Tx-Rx distances. Thus, inspired by the partially absorbing SISO model in [4], where the receiver's contribution outside cone with β is negligible, we introduced three compensation parameters b_i, namely overall scaling b_1 (also called *model fitting*), $4D$ to the power of b_2, and τ to the power of b_3 in y, where τ is time. The cumulative number of molecules in the reception space can therefore be written as [11]:

$$F'(\beta, b_i, \tau) = b_1 \times \frac{R}{d+R} \times \text{erfc}\left(\frac{d}{y'}\right) \times \frac{\Omega(\tau, y', \beta)}{U(\tau, y')}, \tag{2}$$

where $y' = (4D)^{b_2}\tau^{b_3}$ and Ω is [3]:

$$\begin{aligned}\Omega(\tau, y', \beta) = &\frac{1}{d}\text{erfc}\left(\frac{d}{y'}\right) - \frac{1}{x(\beta)}\text{erfc}\left(\frac{x(\beta)}{y'}\right) \\ &+\frac{1}{\sqrt{2\pi D\tau}}\left[\text{Ei}\left(-\frac{d^2}{y'^2}\right) - \text{Ei}\left(-\frac{x^2}{y'^2}\right)\right],\end{aligned} \tag{3}$$

with

$$x(\beta) = \sqrt{(R+d)^2 - 2(R+d)R\cos(\beta) + R^2},$$

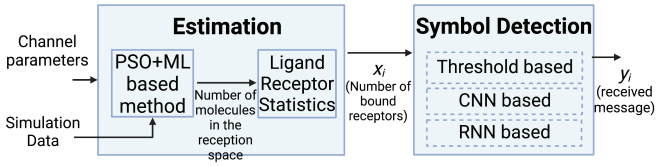

Fig. 2: Illustration of the overall communication model.

and

$$\begin{aligned}U(\tau, y') = &\frac{1}{d}\text{erfc}\left(\frac{d}{y'}\right) - \frac{1}{d+2R}\text{erfc}\left(\frac{d+2R}{y'}\right) \\ &+\frac{1}{\sqrt{D\tau}}\left[\text{Ei}\left(-\frac{d^2}{y'^2}\right) - \text{Ei}\left(-\frac{(d+2R)^2}{y'^2}\right)\right],\end{aligned} \tag{4}$$

in which Ei$(\cdot)$ is exponential integral function.

For the molecular MIMO model, the molecules emitted from a transmitter reach not only the receiver that is aligned with it but also the other receivers of no alignment. That makes the received signal problem physically complex, explaining why no analytical MIMO channel model is available yet. Hence, we propose an additional function, $g(d, h, R, D, \tau)$, to be generated using a regression tree. Using this function, (2) can be rewritten as:

$$\begin{aligned}F''(\beta, b_i, \tau) = &b_1 \times \frac{R}{d'+R} \times \text{erfc}\left(\frac{d'}{y'}\right) \\ &\times \frac{\Omega(\tau, y', \beta)}{U(\tau, y')} \times g(d, h, R, D, \tau),\end{aligned} \tag{5}$$

where d' is the distance between any Tx-Rx pair. The concentration of information molecules, c_s, is calculated by dividing the number of molecules found in (2) by the reception space volume, V, regarding the channel memory.

As mentioned previously, our model considers the effect of ISI and the interference caused by external molecules. Yet, we should also note that the molecules coming from transmitters unaligned with a receiver do not count as interferers. The probability of finding a receptor in the bound state in the presence of interferers with concentration c_{in} is given in [10] as:

$$p(B|S, n_{in}) = \frac{c_s/K_s^D + c_{in}/K_{in}^D}{1 + c_s/K_s^D + c_{in}/K_{in}^D}, \tag{6}$$

where S, c_s, $K_s = k_s^-/k^+$, and $K_{in} = k_{in}^-/k^+$ with $\eta = k_s^-/k_{in}^-$ affinity ratio are respectively the transmitted bit, the concentration of information molecules in the reception space, and the dissociation constants of information and interfering molecules, which give the measures of affinity between a ligand and receptor.

The probability distribution of the number of bound receptors is binomial [10]. Hence, given the number of information and interfering molecules in the reception space, the mean and variance of the number of bound receptors at equilibrium are:

$$\begin{aligned}E(N_B|S, n_{in}) &= p(B|S, n_{in})N_R, \\ Var(N_B|S, n_{in}) &= p(B|S, n_{in})(1 - p(B|S, n_{in}))N_R\end{aligned} \tag{7}$$

where N_R and N_B are the total number of receptors and the bound receptors on a receiver, respectively.

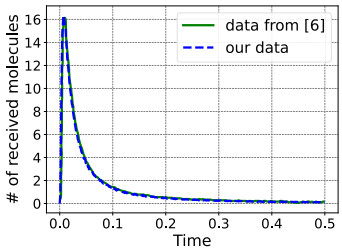

Fig. 3: Comparison of data generated with our simulations and in [6].

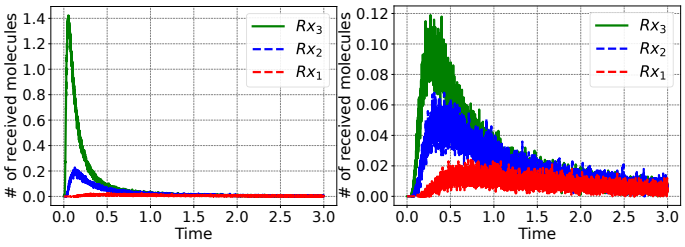

(a) (b)

Fig. 4: Number of received molecules for: a) $d = 4\mu$m, b) $d = 10\mu$m.

Fig. 2 explains the relationships between the inputs we used for estimation, i.e., the channel parameters and simulation data, and shows the role of estimation output, i.e., the number of bound receptors, in symbol detection.

B. Dataset Generation via Simulations

To create a MIMO dataset, we implemented a simulator inspired by [12]. Our simulator was verified by comparing its results with data from [6], and as shown in Fig. 3, the outputs match each other. Fig. 4 reveals that the number of molecules emitted from Tx_i is not significant for Rx_{i+3} or Rx_{i-3}. Hence, in our simulator, we used only one spherical Tx since they are identical, i.e., no need for N of them, and five Rxs. Table II provides the simulation parameters.

As in our previous study [11], we used PSO to find the compensation parameters and the angle of reception in (2). It should be noted that (2) assumes the Tx-Rx pair is aligned due to the SISO consideration; hence, we updated the distance between Rx_i and Tx_j as below:

$$d'_{ij} = \sqrt{(d+R)^2 + |j-i|(2R+h)}. \tag{8}$$

III. Estimation

Here, we estimate the number of molecules and find the number of bound receptors in consideration of the ISI.

TABLE I: Parameter values used in simulations.

Parameter	Value	Unit
# of transmitted molecules	3000	-
# of Rxs	5	-
Simulation time step, ΔT	50	[μs]
Tx-to-Rx distance, d	2, 4, 6, 8, 10	[μm]
Rx-to-Rx distance, h	1, 2, 3	[μm]
Rx radii, R	3, 5, 7	[μm]
Tx radii, r	3, 5, 7	[μm]
Diffusion coefficient, D	50, 100	[μm^2/s]

A. The Number of Received Molecules

To better observe the interactions between Rxs, we selected the case with min. h and R. As Fig. 5 shows, the PSO-based analytical solution for the cumulative number of received molecules cannot estimate the MIMO model well. For the Rx aligned with Tx, i.e., Rx_3 in Fig. 5(a), the error is due to the molecules absorbed by other Rxs. For Rx_2, the difference is more compared to Rx_3, as it is not aligned with Tx, besides due to the absorption of other Rxs. This effect can also be seen for Rx_1 in Fig. 5(c). Lastly, the number of received molecules with increasing d is not as clear as Rx_1 or Rx_3 for Rx_2.

We generated the $g(\cdot)$ dataset in (5) by dividing the simulation data into the outputs resulting from the updated version of (2), where Fig. 6 visualizes the output of this function. Yet, suggesting an analytical equation for $g(\cdot)$ is not easy. Hence, we trained a regression tree, i.e., a supervised learning model. To handle overfitting, we used cross-validation, giving a better estimate of the trained model performance.

Fig. 7 shows the RMSE performance of our solution for the number of received molecules, in which $d = 2\,\mu$m is not considered since it converges to SISO, i.e., most of the emitted molecules are received by Rx_3, as shown in Fig. 5. For other distances, the performance is affected by the total number of molecules at the reception space of Rxs. Thus, Rx_2 and Rx_3 perform better with increasing d. For Rx_1, the RMSE is more stable, as it is far from the emission point of molecules, i.e., the emission spike affects Rx_1 less compared to other Rxs.

B. Ligand Receptor Binding

Estimating the information molecule concentration in the reception space is vital for an accurate bound receptor analysis. With $\Delta T = 5\times10^{-4}$sec, the symbol slots are of length $n\Delta T$ with channel length, n, having different integer values. For a given ISI window, the number of received molecules at the m^{th} symbol slot is the sum of Binomial distributed random variables, where each summand denotes the number of hitting molecules due to a previous emission, accounting for the ISI.

Here, we consider an ISI window of η. For the m^{th} symbol:

$$c_s = \frac{1}{V}\sum_{k=0}^{\eta} N s^{Tx}_{m-k} F[k], \tag{9}$$

where V, N, and s^{Tx} are the reception space volume, the number of transmitted molecules, and the transmitted symbol, respectively. We found the number of bound receptors using (7) and the parameters provided in Table II.

TABLE II: Parameter values for ligand-receptor interactions.

Parameter	Value	Unit
Binding rate for both types of molecules (k^+)	2×10^{-17}	[m^3/s]
Unbinding rate for information molecules (k_s^-)	10	[s^{-1}]
Affinity ratio (η)	0.2	-
Mean concentration of interferer molecules	$2\times K_D^{in}$	-
# of receptors on the receiver surface	10000	-
Thickness of the reception space	1	[μm]

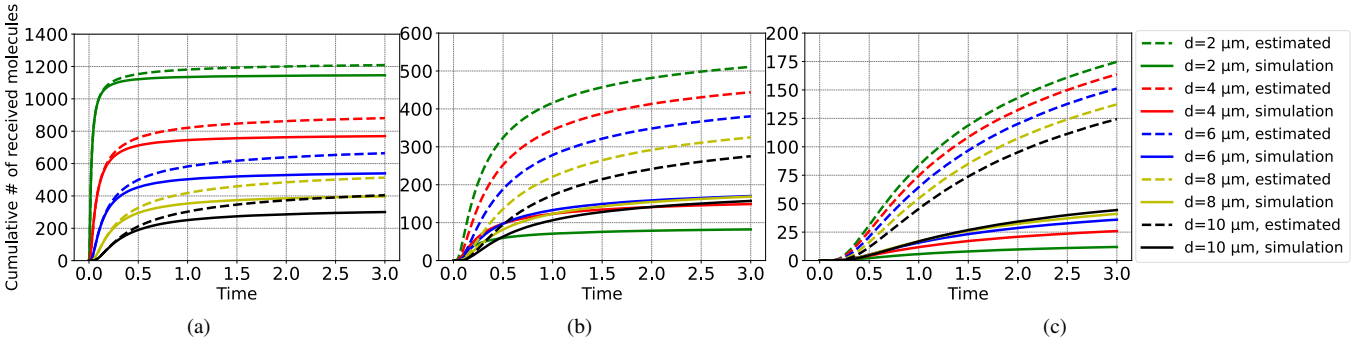

(a) (b) (c)

Fig. 5: Comparison between the analytical solution of (2) and the cumulative simulation data for: a) Rx_3, b) Rx_2, and c) Rx_1.

IV. Symbol Detection

For detecting the incoming messages, we used the number of bound receptors (DNBR). The decision is made by sampling the number of bound receptors as $\hat{s} = \text{argmax}_{s\in\{0,1\}}\, p(N_B|s)$. For the binary-CSK modulation scheme, the incoming message can be mapped with detection thresholds, i.e.: $N_B \lessgtr_{H1}^{H0} \xi$. Next, we explain the detection methods evaluated in this study.

A. Detection Methods

1) Threshold-based Detection: The detection threshold minimizing the error of a Binary Shift Keying (BSK)-modulated transmission is [10]:

$$\xi = \gamma^{-1} \times (Var[N_B|s=1]E[N_B|s=0] - Var[N_B|s=0]E[N_B|s=1] + Std[N_B|s=1]Std[N_B|s=0] \times \sqrt{E[N_B|s=1] - E[N_B|s=0] + 2\gamma \ln \frac{Std[N_B|s=1]}{Std[N_B|s=0]}}), \tag{10}$$

where $\gamma = Var[N_B|s=1] - Var[N_B|s=0]$.

Table III provides the BER of the case with $d = 8\mu$m, $h = 1\mu$m, $R = 3\mu$m, and $D = 50\mu\text{m}^2/\text{s}$. Finding the minimum BER for each possible threshold gives the optimal BER values, while the calculated ones are based on (10). The difference between them is due to the imperfect normal distribution, as Fig. 8 shows, where 10^5 bits were transmitted considering the interferers. The region overlapping for bit-0 and bit-1 in Fig. 8 is inevitable due to the ISI. Hence, a decision rule that is more complicated than the optimal threshold is required for DNBR to achieve a lower error.

2) CNN-based Detection: In the presence of ISI, we used the received signals of multiple symbols as inputs of a CNN. The symbol detector consists of the following three layers: *Input layer* holds the estimated number of bound receptors. *Convolutional layer* determines the output of neurons connected to local regions of the input by calculating the scalar product between their weights and the regions connected to the input volume. Since our input signal is a sequence, we use a one-dimensional (1D) convolutional layer. The loss function, optimizer function, learning rate, batch size, and epoch number are selected as binary cross-entropy, Adam Algorithm, 0.01, 64, and 30, respectively. *Fully-connected layer* performs the same duties as standard ANNs and attempts to produce class scores from activations to be used for classification.

3) RNN-based Detection: Unlike CNN and standard ANN, the Recurrent Neural Network (RNN) has feedback connections, i.e., it is useful for time-dependent models like ours. In RNN, the input shape of data depends on the model's channel memory. Considering the simulation time and the peak signal time of the channel, we set η to 4, giving the maximum ISI.

TABLE III: Minimum BER comparison of the optimal values with the calculated ones using (10) for threshold-based detection.

	Rx_1	Rx_2	Rx_3
Optimal BER	0.11914	0.11269	0.04633
Calculated BER	0.14114	0.14873	0.07818

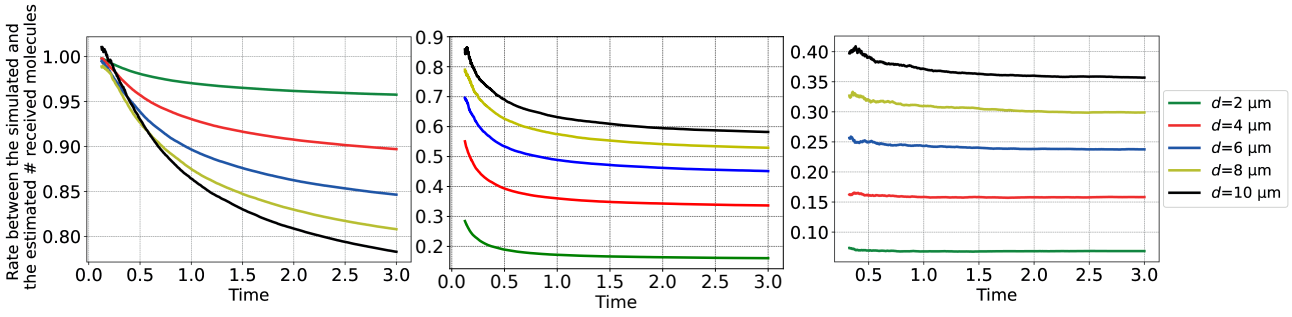

(a) (b) (c)

Fig. 6: Rates between the simulated data and the estimated number of received molecules based on (2) for: a) Rx_3, b) Rx_2, and c) Rx_1

.

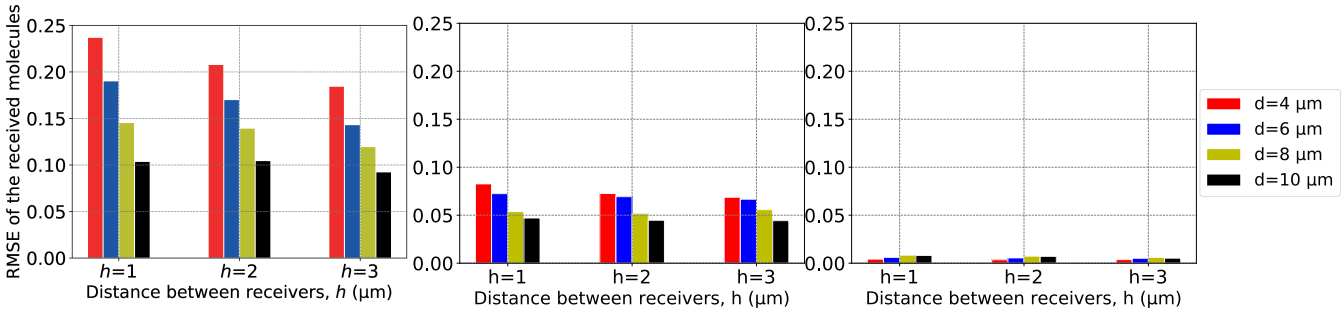

(a) (b) (c)

Fig. 7: RMSE performance of the regression model for: a) Rx_3, b) Rx_2, and c) Rx_1.

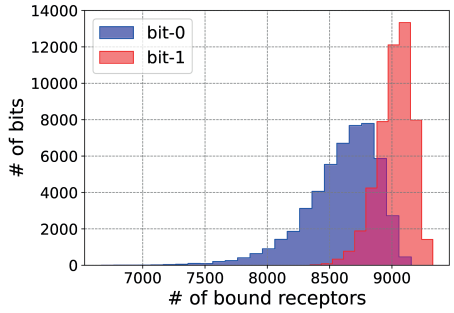

Fig. 8: Relation between the number of received bits and the number of bound receptors for Rx_1.

For this detection method, instead of the 1D convolutional layer in Sec. IV-A2, we used a four-unit long short-term memory (LSTM) layer. The LSTM architecture aims to provide a short-term memory for the RNN that can last many timesteps.

B. BER Comparison

For the BER comparison of the proposed detection methods, we investigated the cases with high ISI and optimum channel length since detection gets harder with decreasing sampling duration and increasing channel memory. The results summarized in Table IV reveal the following: *i)* both CNN- and RNN-based methods outperform the basic threshold-based decision; *ii)* the neural network-based methods improve the BER, especially for short d; *iii)* the convolutional layer returns better BER results compared to that of the time-dependent LSTM layer; and *iv)* CNN-based method improves the mean BER three times compared to its threshold-based counterpart.

TABLE IV: BER comparison of threshold-, RNN-, and CNN-based symbol detection for 10^6 bits at different Tx-Rx distances, d.

	2μm	4μm	6μm	8μm	10μm
Threshold-based	0.1365	0.1598	0.1724	0.1859	0.1941
RNN-based	0.0312	0.0976	0.1398	0.1765	0.1914
CNN-based	0.0045	0.0112	0.0260	0.0750	0.1460

V. Conclusions

Using a regression tree for the non-analytical nature of MIMO channels, besides the parameter searching with PSO, gave us good RMSE performance. For varying d and h values, the RMSEs were consistent. Using the estimation output, we analyzed the detection based on BNBR under the presence of ISI and molecular interference for ligand receptors. The results showed that the generic threshold-based technique was insufficient when different symbols overlap. Hence, we proposed two new detectors based on CNN and RNN. These data-driven models outperformed the generic technique, especially for small d values. Also, the mean BER was improved three times with the CNN-based detector compared to that of the threshold-based one. We would like to note that these networks have no multiple layers; therefore, they are computationally more efficient than a deep neural network algorithm. Hence, such more developed techniques can be helpful for interference-affected MIMO models in IoBNT, especially when binding reactions exist between the transmitted molecules and the receivers with ligand receptors.

References

[1] I. F. Akyildiz *et al.*, "The internet of bio-nano things," *IEEE Communications Magazine*, vol. 53, no. 3, pp. 32–40, 2015.
[2] O. B. Akan *et al.*, "Fundamentals of molecular information and communication science," *Proc. IEEE*, vol. 105, no. 2, pp. 306–318, 2017.
[3] B. C. Akdeniz *et al.*, "Molecular signal modeling of a partially counting absorbing spherical receiver," *IEEE Trans. Commun.*, vol. 66, no. 12, pp. 6237–6246, 2018.
[4] H. B. Yilmaz*et al.*, "A machine learning approach to model the received signal in molecular communications," in *IEEE BlackSeaCom*, 2017, pp. 1–5.
[5] X. Qian and M. Di Renzo, "Receiver design in molecular communications: An approach based on artificial neural networks," in *IEEE ISWCS*, 2018, pp. 1–5.
[6] C. Lee *et al.*, "Machine learning based channel modeling for molecular mimo communications," in *IEEE SPAWC*, 2017, pp. 1–5.
[7] N. Farsad *et al.*, "Data-driven symbol detection via model-based machine learning," in *IEEE Statistical Signal Proc. Workshop*, 2021, pp. 571–575.
[8] M. Kuscu *et al.*, "Transmitter and receiver architectures for molecular communications: a survey on physical design with modulation, coding, and detection techniques," *Proc. IEEE*, vol. 107, no. 7, pp. 1302–1341, 2019.
[9] C. A. Söldner *et al.*, "A survey of biological building blocks for synthetic molecular communication systems," *IEEE Communications Surveys & Tutorials*, vol. 22, no. 4, pp. 2765–2800, 2020.
[10] M. Kuscu and O. B. Akan, "Detection in molecular communications with ligand receptors under molecular interference," *Digital Signal Processing*, vol. 124, p. 103186, 2022.
[11] A. Das *et al.*, "Received signal modeling and ber analysis for molecular siso communications," in *The Ninth Annual ACM International Conference on Nanoscale Computing and Communication (NANOCOM '22)*, 2022.
[12] H. B. Yilmaz, "MolecUlar CommunicatIoN (MUCIN) simulator," MATLAB Central File Exchange [Online]. Available: https://www.mathworks.com/matlabcentral/fileexchange/4606-molecular-communication-mucin-simulator, 2020.